# A novel anti-atherosclerotic mechanism of quercetin: Competitive binding to KEAP1 via Arg483 to inhibit macrophage pyroptosis

Xing Luo [a,b,1], Xiuzhu Weng [a,b,1], Xiaoyi Bao [a,b,1], Xiaoxuan Bai [a,b], Ying Lv [a,b], Shan Zhang [a,b], Yuwu Chen [a,b], Chen Zhao [a,b], Ming Zeng [a,b], Jianxin Huang [a,b], Biyi Xu [a,b], Thomas W. Johnson [c], Stephen J. White [d], Ji Li [a,b,*], Haibo Jia [a,b,*], Bo Yu [a,b]

[a] *Department of Cardiology, The 2nd Affiliated Hospital of Harbin Medical University, Harbin, 150001, PR China*
[b] *Key Laboratory of Myocardial Ischemia, Chinese Ministry of Education, Harbin, 150001, PR China*
[c] *Department of Cardiology, Bristol Heart Institute, Upper Maudlin St., Bristol, BS2 8HW, UK*
[d] *Department of Life Sciences, Manchester Metropolitan University, Manchester, M1 5GD, UK*

## ARTICLE INFO

## ABSTRACT

Natural antioxidants represented by quercetin have been documented to be effective against atherosclerosis. However, the related mechanisms remain largely unclear. In this study, we identified a novel anti-atherosclerotic mechanism of quercetin inhibiting macrophage pyroptosis by activating NRF2 through binding to the Arg483 site of KEAP1 competitively. In ApoE$^{-/-}$ mice fed with high fat diet, quercetin administration attenuated atherosclerosis progression by reducing oxidative stress level and suppressing macrophage pyroptosis. At the cellular level, quercetin suppressed THP-1 macrophage pyroptosis induced by ox-LDL, demonstrated by inhibiting NLRP3 inflammasome activation and reducing ROS level, while these effects were reversed by the specific NRF2 inhibitor (ML385). Mechanistically, quercetin promoted NRF2 to dissociate from KEAP1, enhanced NRF2 nuclear translocation as well as transcription of downstream antioxidant protein. Molecular docking results suggested that quercetin could bind with KEAP1 at Arg415 and Arg483. In order to verify the binding sites, KEAP1 mutated at Arg415 and Arg483 to Ser (R415S and R483S) was transfected into THP-1 macrophages, and the anti-pyroptotic effect of quercetin was abrogated by Arg483 mutation, but not Arg415 mutation. Furthermore, after administration of adeno associated viral vector (AAV) with AAV-KEAP1-R483S, the anti-atherosclerotic effects of quercetin were almost abolished in ApoE$^{-/-}$ mice. These findings proved quercetins suppressed macrophage pyroptosis by targeting KEAP1/NRF2 interaction, and provided reliable data on the underlying mechanism of natural antioxidants to protect against atherosclerosis.

## 1. Introduction

Atherosclerosis is a kind of chronic inflammatory disease characterized by plaque formation, in which macrophages are the main pro-inflammatory cells [1]. Pathological studies have found abundant dead macrophages in vulnerable plaques [2], and there is accumulating evidence that macrophage death triggers inflammatory responses leading to plaque instability [3]. Thus, inhibition of macrophage death may contribute to preventing atherosclerotic plaques progression and destabilization.

Pyroptosis is a pro-inflammatory form of programmed cell death. The distinctive features of pyroptosis included membranolysis and the leakage of intracellular contents, such as high mobility group box 1, lactate dehydrogenase (LDH), and cytokines [4–6]. In macrophages, pyroptosis is triggered by NLRP3 inflammasome activation and cleavage of caspase1 (cle-caspase1) [7–9]. N-terminal Gasdermin D (N-GSDMD)

activated by cle-caspase1 migrates to the plasma membrane and forms pores, leading to pyroptosis [5,10,11]. Recently, several studies have shown that pyroptosis plays an important role in the progression of atherosclerosis [12]. Autopsy studies revealed that, compared to normal vessels, the expression of NLRP3 and caspase1, the major component of NLRP3 inflammasome, are significantly higher in atherosclerotic plaques, and also correlates with the markers of plaque instability [13,14]. It was found that caspase1 deletion significantly attenuated atherosclerotic plaque progression in ApoE$^{-/-}$ mice [15,16]. Moreover, MCC950, a specific NLRP3 inhibitor, was reported to protect against atherosclerosis effectively [11]. However, as the main inflammatory cell in plaque, the underlying mechanisms of macrophage pyroptosis in atherosclerosis remain to be elucidated [17].

There is increasing evidence that oxidative stress is an activator of NLRP3 inflammasome. The excessive cellular ROS has been proved to be a common trigger for NLRP3 inflammasome formation and pyroptosis. Furthermore, several reactive oxygen scavengers also have been reported to effectively suppress pyroptosis by inhibiting inflammasome activation [18–20]. For instance, inhibition of NADPH oxidase-derived ROS prevented ATP-induced caspase1 activation and pyroptosis in alveolar macrophages [21]. Moreover, it was also reported that ROS can directly cause pyroptosis independently of NLRP3 inflammasome by directly activating GSDMD [22]. Since oxidative stress plays an important role in pyroptosis, natural antioxidants can be used as candidates for the treatment of pyroptosis-related diseases. As a classical natural antioxidant, quercetin is well recognized for its multiple biological functions including anti-oxidation and anti-inflammation. Previous studies have reported that quercetin has a protective effect on atherosclerosis, including inhibition of dendritic cell activation and excessive ROS production [23,24]. Moreover, our *in vitro* study supported that quercetin improved oxidative stress in pyroptotic macrophages induced by LPS/ATP [25]. In this study, we will further elucidate the potential mechanisms by which quercetin ameliorates oxidative stress.

KEAP1/NRF2 is a common protein complex which regulates the expression of numerous antioxidant genes that preserve cellular oxidative stress homeostasis. Under physiological conditions, KEAP1 binds to NRF2 in cytoplasm, leading to ubiquitination and degradation of NRF2 [26]. When cells are exposed to oxidative stress, NRF2 will be released into the nucleus, where it could bind to antioxidant response elements, eventually leading to transcription of antioxidant proteins [26,27]. Previous studies have confirmed that quercetin inhibits oxidative stress by activating the NRF2 pathway [28]. However, the detailed mechanisms of NRF2 activation by quercetin and its role in atherosclerosis remain unclear.

In the present study, we investigated the protective effect of quercetin on macrophage pyroptosis in atherosclerotic plaques and elucidated the underlying mechanisms of NRF2 activation by quercetin. Our results provide new insights into the mechanisms of natural antioxidants in the treatment of atherosclerosis.

## 2. Materials and methods

### 2.1. Animal experiments and tissue harvest

All animal experimental procedure protocols were approved by the institutional research ethics committee of the Second Affiliated Hospital of Harbin Medical University, and procedures were performed in accordance with the National Institutes of Health guidelines (Guide for the Care and Use of Laboratory Animals) and the guidelines from Directive 2010/63/EU of the European Parliament on the protection of animals used for scientific purposes.

6–8 weeks male ApoE$^{-/-}$ mice with a C57BL/6 background were purchased from Beijing Vital River Laboratory Animal Technology (Beijing, China) and housed in the animal center of Harbin Medical University (22 $\pm$ 2 °C, 55 $\pm$ 5% relative humidity with a 12 h light/dark cycle). The mice were free to food and water. These mice were randomly

divided into three groups with different diets for 16 weeks: normal chow diet (ND), high fat western type diet (21% fat, 0.15% cholesterol; MD12015; Medicine Ltd., Jiangsu, China) (HD); and high fat western type diet supplemented with 0.1% quercetin (Quer) according to previous study [29]. During the experiment time, blood glucose, body weight and the food uptake were recorded every two weeks. After 16 weeks, all animals were anesthetized with an intraperitoneal injection of sodium pentobarbital (50 mg/kg body weight) and then euthanized by cervical dislocation. The plasma was collected and frozen immediately. The hearts and aortas were removed carefully and fixed with 4% paraformaldehyde (4 °C for 24 h) or kept in optimal cutting temperature compound (OCT) for immunostaining.

### 2.2. Reagents

The following drugs and reagents were used in the present study: quercetin (C$_{15}$H$_{10}$O$_7$, 98% purity), was obtained from Chengdu Herbpurify (Chengdu, China). Ox-LDL was purchased from Yiyuan Biotechnology (Guangzhou, China). SYBR Green and Reverse Transcription kit were obtained from Roche (Basel, Switzerland). Primary antibody sources are as follows: antibodies against NLRP3 (D4D8T), caspase1 (D7F10), N-GSDMD (93709), cle-caspase1 (D57A2), NRF2 (D1Z9C), Heme oxygenase-1(HO-1) (E9H3A), KEAP1 (P586) and IL-1β (D3U3E) were purchased from Cell Signaling Technology (Boston, USA), antibody against β-actin and Goat anti-rabbit antibody were obtained from Merck (Darmstadt, Germany). Lipid Peroxidation MDA Assay Kit, ROS Assay Kit, Total Superoxide Dismutase Assay Kit with NBT, LDH Cytotoxicity Assay Kit and Apoptosis and Necrosis Assay Kit are obtained from Beyotime Biotechnology (Shanghai, China). Enzyme linked immunosorbent assay (ELISA) kits for IL-1β and IL-18 was obtained from Ebioscience (Wuhan, China).

### 2.3. Cell culture and treatment

Human myelomonocytic THP-1 cells (ATCC, USA) were cultured in RPMI 1640 medium (Gibco, USA), supplemented with 10% fetal bovine serum (Gibco, USA) and 1% penicillin (Beyotime, China). Cell culture medium was renewed every 2 days, and the cultures were maintained at 37 °C, 95% air/5% CO$_2$ in a fully humidified incubator. Before each experiment, THP-1 cells were differentiated into macrophages by treatment with 50 nM phorbol myristate acetate (PMA) for 48 h [30]. Macrophages were pretreated with quercetin (50 μM) for 1 h, then stimulated with 100 μg/ml ox-LDL for 24 h.

### 2.4. Cell viability assay

Cell viability was detected using enhanced cell counting kit-8 (CCK-8) (Dojindo, Japanese). After treatment, 100 μl CCK-8 working solution was added into each well of the 96-plate and incubated with the macrophage for 2 h at 37 °C, before reading the optical density of each well at 450 nm using a microplate reader.

### 2.5. LDH assay

Briefly, macrophages were cultured into 96-well plates, and treated with 100 μg/ml ox-LDL for 24 h with or without 50 μM quercetin pretreatments for 1 h. The maximum LDH release control was created by the addition of 20 μl 10 × lysis solution 45 min before performing the assay. 120 μl of culture supernatant was transferred to a new 96-well plate, and 60 μl working solution was added to each well, incubated for 25 min at room temperature in the dark, before reading the absorbance at 490 nm.

### 2.6. Real-time reverse transcription-PCR

Total RNA was isolated from treated THP-1 using Trizol regent

according to the manufacturer's instructions (Invitrogen, USA). cDNA was synthesized using the Reverse Transcription kit (Roche, Switzerland), and quantitative polymerase chain reaction (qPCR) performed using SYBR Green (Roche, Switzerland). The mRNA expressions of NLRP3, caspase1 and IL-1β was quantified. Using primers were listed in the Supplemental Table 1. All data was normalized to the mRNA expression level of β-actin.

### 2.7. Cytoplasmic DNA isolation and mtDNA copy number analysis

Mitochondria were extracted from macrophage by using the Mitochondria Isolation Kit (Beyotime, China) according to the manufacturer's instructions, to allow the extraction of nuclear DNA (nDNA) and mitochondrial DNA (mtDNA) by using the genomic DNA miniprep kit (Axygen, USA). The short regions of the tRNA-Leu$^{UUR}$ and β2-microglobulin genes were used to quantify mtDNA and nDNA respectively, from which the mtDNA/nDNA ratio was calculated to determine the mtDNA copy number as previously described [31].

### 2.8. Hoechst/propidium iodide (PI) staining

Hoechst/PI staining was performed according to the manufacturer's instructions. Treated THP-1 cells were carefully washed twice by ice-cold PBS, then stained with PI (2 μg/ml; staining for membrane damaged cells) and Hoechst (5 μg/ml; nuclear counterstain for all cells) at 4 °C for 30 min. Cells were then washed once more in ice-cold PBS and observed under a fluorescent microscope (OLYMPUS, Japan).

### 2.9. Western blot and immunoprecipitation

Total protein from treated THP-1 cells or mouse tissue were extracted by using lysing buffer (Roche, Switzerland). Anti-KEAP1 (1:50) or normal rabbit IgG (1:50) control was added to the supernatants and incubated at 4 °C overnight for immunoprecipitation. Antibody pull down was performed by incubation with of 40 μl of protein A magnetic (Bimake, USA). Agarose beads for 5 h at 4 °C, followed by magnetic pull down and 3 wash steps. Proteins were eluted by heating at 95 °C for 5 min. Protein concentration was measured by BCA Protein Assay Kit (Beyotime, China). Equal amount of protein (40 μg) was separated by SDS polyacrylamide gel electrophoresis and transferred onto 0.22 μm PVDF membranes (Millipore Corporation, USA). Membranes were blocked with 5% skim milk for 1 h at room temperature with sustained shaking. Thereafter, membranes were incubated with antibody at 4 °C overnight. Membranes were washed and incubated with secondary antibodies for 1 h at room temperature with sustained shaking. Protein bands were visualized by ECL reagent (Beyotime, China).

### 2.10. Measurement of mitochondrial and intracellular oxidative stress levels

The total and mitochondrial ROS level were detected by Dichlorodihydrofluorescein diacetate (DCFH-DA) (Beyotime, China) and mitosox red mitochondrial superoxide indicator (ThermoFisher, USA) according to manufacturer's instructions. Briefly, treated THP-1 macrophages were washed twice with cold PBS and incubated with DCFH-DA or mitosox at room temperature for 30 min in the dark. Following two additional cold PBS washes, the intensity of fluorescence was determined by fluorescent microscopy. Malondialdehyd (MDA), glutamylcysteinyl-glycine (GSH) level and superoxide dismutase (SOD) activity in cell homogenate and serum in ApoE$^{-/-}$ mice were measured according to manufacturer's instructions (Beyotime, China). All experiments were repeated three times.

### 2.11. Immunofluorescent staining

Treated THP-1 macrophages, plated on glass slides, or 8 μm sections

mouse tissues were washed twice by PBS and incubated with cold acetone for 10 min. The macrophages/tissues were washed with PBS three times. 0.1% Triton was used to break down cell membranes. Macrophages/tissues were blocked with 5% bovine serum albumin for 1 h at room temperature, then macrophages/tissues were washed with PBS three times again. After that, the macrophages/tissues were incubated with antibody at 4 °C overnight, followed by incubating with secondary antibodies (1:200) for 1 h at room temperature. Ultimately, the macrophages/tissues were incubated with DAPI for 3 min and observed by fluorescent microscope.

### 2.12. Histopathologic and TdT-mediated dUTP nick-end labeling (Tunel) staining

The artery tissue from mice and patients were fixed in 4% paraformaldehyde at 4 °C and processed for paraffin embedding and fresh frozen or OCT embedding, respectively. According to the requirements of the experiment, the paraffin slicer was used to cut the tissue continuously. 8 μm sections were cut throughout the tissue every 3 section. The Oil Red-O (OCT embedding), Masson and Tunel stain are performed according to manufacturer's instructions (Roche, Switzerland).

### 2.13. Plasmid transfection

The mammalian expression plasmids containing KEAP1-WT, or KEAP1 with single mutations at R415S or R483S were purchased from HanBio Tech (Shanghai, China). Adeno associated viral vector (AAV) with R483S was purchased from HanBio Tech (Shanghai, China). Amino acid mutation sequences were shown in Supplemental Table 2. The macrophages were transfected using Lipo3000 reagent (Invitrogen, USA), according to the manufacturer's instructions. Briefly, 2 μl Lipo3000 reagent and 2 μl plasmid (0.8 μg) were diluted into 50 μl Opti-MEM and incubated at room temperature for 5 min before mixing and incubation for a further 20 min. Following incubation, the transfection mixture was added to 50 nM PMA treated THP-1 cells in a 24-well plate. Cells were assayed after 48 h.

### 2.14. Molecular docking analysis

The structure of quercetin (PubChem CID 5280343) was obtained from the PubChem database (https://pubchem.ncbi.nlm.nih.gov/). The crystal structure of the KEAP1 protein combined with NRF2 protein (PDB code: 2FLU) was acquired from the RCSB Protein Data Bank (https://www.rcsb.org/). The energy of quercetin was minimized using the MMFF2 force field with the Powell conjugate gradient minimization algorithm and a convergence criterion of 0.005 kcal/(mol•A). Subsequently, the NRF2 protein was removed from the 2FLU structure to expose site of interaction on the crystal structure of the KEAP1 protein involved in docking with NRF2. The hydrogen atoms were then added to the KEAP1 protein structure to prepare the structure for docking experiments, along with removal of water from the protein structure. DS 2.5 was then used to define the active site of the KEAP1 crystal structure and calculate the docking site, which is covered with a grid box sized 18.6 Å × 18.6 Å × 18.6 Å. Quercetin was set as the ligand for KEAP1 protein, and the molecular docking was performed at different binding ratios using the lib-Dock method [32]. The docking energies were obtained to evaluate the docking affinity of quercetin to KEAP1.

### 2.15. Statistical analysis

All the results were presented as mean ± standard error of mean, and all the data were acquired from at least three independent experiments. Two-tailed Student's t-test were used to compare data between two groups with normal distributed values. Mann-Whitney *U* test was used to compare data between two groups with non-normal distributed values. Statistical analysis was performed using SPSS 21.0 software. P < 0.05

was considered statistically significant.

## 3. Results

### 3.1. Quercetin attenuated the progression of atherosclerosis in ApoE$^{-/-}$ mice

6–8 weeks male ApoE$^{-/-}$ mice were randomly divided into three groups, a normal diet (ND) group, high fat diet (HD) group and HD supplemented with 0.1% (w/w) quercetin (Quer) group. HE and Oil Red-O staining were used to evaluate plaque area and lipid deposition of the aortic root among the three groups. These results indicated that quercetin significantly decreased plaque area and the lipid deposition (Fig. 1A–C). The content of collagen was closely related to plaque stability, Masson staining indicated that quercetin significantly increased the content of collagen (Fig. 1A and D). Taken together, the data demonstrated that quercetin inhibited atherosclerosis plaque progression in ApoE$^{-/-}$ mice.

The baseline of these mice was also recorded during the experiment. After 16 weeks, the mice of HD and Quer group showed higher weight than those of ND group, but no significant difference was observed between HD and Quer group (Supplemental Fig. 1A). To examine whether quercetin influences appetite of mice, the average daily food intake of each mouse was recorded. The result demonstrated that there was no significant difference in the food intake of mice among ND, HD and Quer group (Supplemental Fig. 1C). Fasting blood-glucose was monitored every two weeks, no significant differences were observed between the mice of different groups (Supplemental Fig. 1B). Total cholesterol (TC), triglyceride (TG), LDL-C, and HDL-C levels were measured at the end of the 16-week feeding protocol. The results showed that serum TC, TG, and LDL-C levels were higher in HD group, while HDL-C was lower. Compared to HD group, quercetin significantly reduced TC, TG and LDL-C levels in serum, and increased the HDL-C level (Fig. 1E–H).

### 3.2. Macrophage pyroptosis was a feature of atherosclerotic plaques in ApoE$^{-/-}$ mice and was reduced by quercetin

Macrophage death has been shown to play an important role in the progression of atherosclerotic plaques. As shown in Fig. 2A, the Mac-3 positive staining area (in red) displayed the macrophage infiltration in plaque. Moreover, there was higher Tunel and Mac-3 double positive area in the aortic root of HD group than ND group, while this effect was attenuated by quercetin (Fig. 2B). To further investigate the form of macrophage death in plaques and the potential mechanism of quercetin protection against atherosclerosis, we performed Mac-3/NLRP3 and Mac-3/caspase1 double staining to indicate co-localization of NLRP3 and caspase1 in macrophage. Quercetin markedly decreased the NLRP3 and caspase1 expression in plaque (Fig. 2C–F). Western blot analysis of lysed aorta demonstrated that the expression of NLRP3, cle-caspase1, N-GSDMD, IL-18, and IL-1β were all elevated in HD group, which were normalized by quercetin (Fig. 2H and I). Consistent with inflammasome activation in HD group, serum IL-1β and IL-18 levels were significantly increased, which was also reversed by quercetin in comparison with the HD group (Fig. 2G). These results provided evidence that macrophage pyroptosis is a feature in atherosclerotic plaques and that quercetin is able to suppress macrophage pyroptosis in this context.

### 3.3. Ox-LDL induction of NLRP3 inflammasome mediated pyroptosis in THP-1 macrophage was inhibited by quercetin treatment in vitro

In order to confirm the inhibitory effect of quercetin on macrophage pyroptosis in vitro, ox-LDL was used to induce THP-1 macrophage pyroptosis. Cell swelling is a key characteristic of pyroptosis, and it can be observed obviously from scanning electron microscope (SEM) that ox-LDL treatment induced cell swelling, while this change was ameliorated by quercetin treatment (Fig. 3A and B). Cell membrane discontinuity is also a feature of cell pyroptosis, which results in positive PI staining, loss of viability and increase in LDH release from the cytoplasm into the supernatant. Ox-LDL treatment induced a significant increase in percentage of PI positive macrophages, reduction in viability (assayed by CCK-8 quantification) and increase in LDH release, all of which were
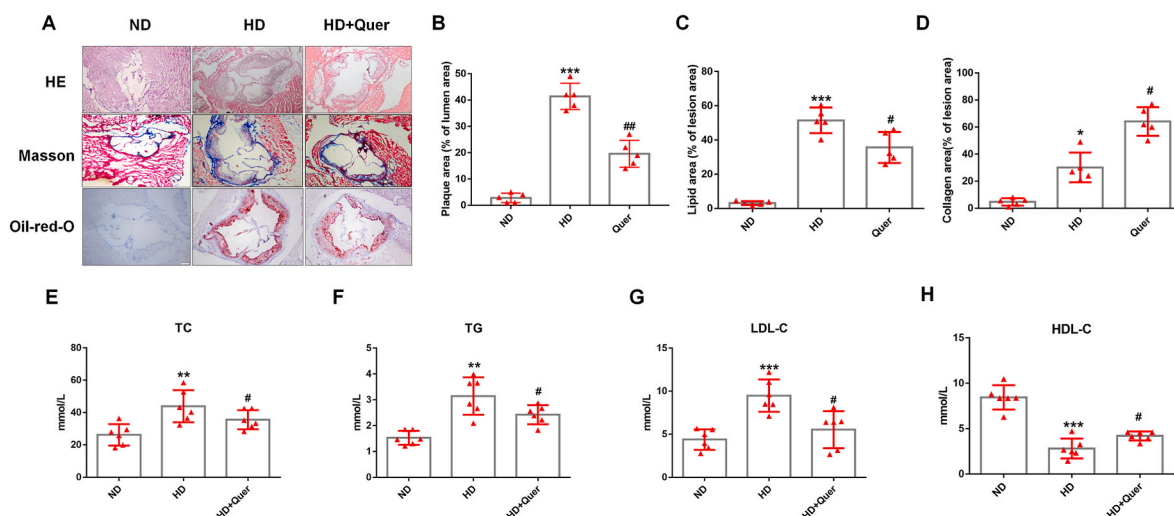


**Fig. 1.** Quercetin oral administration attenuates the progression of atherosclerosis and improves the lipid metabolism in ApoE$^{-/-}$ mice. Animals are divided into: ND group, HD group and HD + Quer group. After the experiment, the tissue is harvested and stained with HE, Masson and Oil red O, the serum is collected to analyze the TG, TC, LDL-C, and HDL-C levels. (A). Representative images for HE, Masson, and Oil red O stain. (B). Quantized data for HE stain (n = 5 ND vs n = 5 HD, ***p < 0.001. n = 5 HD vs n = 5 HD + Quer, ##p < 0.01). (C). Quantized data for Oil red stain (n = 5 ND vs n = 5 HD, ***p < 0.001. n = 5 HD vs n = 5 HD + Quer, #p < 0.05). (D). Quantized data for Masson stain (n = 5 ND vs n = 5 HD, *p < 0.05. n = 5 HD vs n = 5 HD + Quer, #p < 0.05). (E). TC level in serum (n = 6 ND vs n = 6 HD, **p < 0.01. n = 6 HD vs n = 6 HD + Quer, #p < 0.05). (F). TG level in serum (n = 6 ND vs n = 6 HD, **p < 0.01. n = 6 HD vs n = 6 HD + Quer, #p < 0.05). (G). LDL-C level in serum (n = 6 ND vs n = 6 HD, ***p < 0.001. n = 6 HD vs n = 6 HD + Quer, #p < 0.05). (H). HDL-C level in serum (n = 6 ND vs n = 6 HD, ***p < 0.001. n = 6 HD vs n = 6 HD + Quer, #p < 0.05). . (For interpretation of the references to colour in this figure legend, the reader is referred to the Web version of this article.)
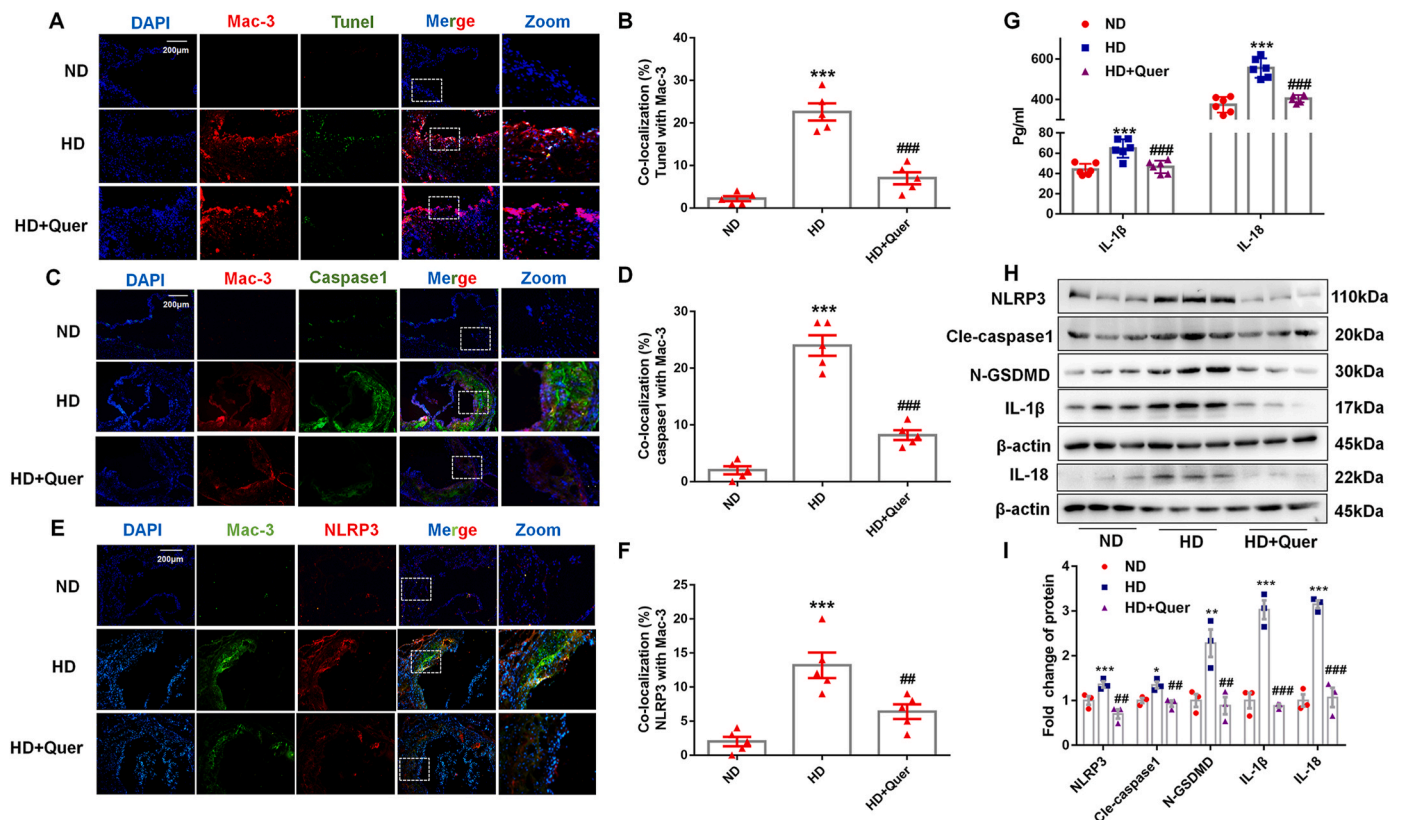
**Fig. 2.** Quercetin oral administration suppresses the NLRP3 inflammasome and alleviates the pyroptosis of macrophages in ApoE$^{-/-}$ mice.
(A, B). Tunel and Mac-3 co-staining in aortic sinus (n = 5 ND vs n = 5 HD, ***p < 0.001. n = 5 HD vs n = 5 HD + Quer, ###p < 0.001). (C, D). Caspase1 and Mac-3 co-staining in aortic sinus (n = 5 ND vs n = 5 HD, ***p < 0.001. n = 5 HD vs n = 5 HD + Quer, ###p < 0.001). (E, F). NLRP3 and Mac-3 co-staining in aortic sinus (n = 5 ND vs n = 5 HD, ***p < 0.001. n = 5 HD vs n = 5 HD + Quer, ##p < 0.01). (G). IL-1β and IL-18 level in ApoE$^{-/-}$ mice serum (n = 6 ND vs n = 6 HD, ***p < 0.001. n = 6 HD vs n = 6 HD + Quer, ###p < 0.001). (H, I). The protein levels of NLRP3 (n = 3 ND vs n = 3 HD, ***p < 0.001. n = 3 HD vs n = 3 HD + Quer, ##p < 0.01), cle-caspase1 (n = 3 ND vs n = 3 HD, *p < 0.05. n = 3 HD vs n = 3 HD + Quer, 0.7-fold change, ##p < 0.01), N-GSDMD (n = 3 ND vs n = 3 HD, **p < 0.01. n = 3 HD vs n = 3 HD + Quer, ##p < 0.01), IL-18, and IL-1β (n = 3 ND vs n = 3 HD, ***p < 0.001. n = 3 HD vs n = 3 HD + Quer, ##p < 0.01) and in the aorta of ApoE$^{-/-}$ mice.

reversed by quercetin treatment (Fig. 3C–F). Western blot quantification of the expressions of NLRP3, cle-caspase1, IL-18, IL-1β and N-GSDMD, demonstrated that ox-LDL treatment increased the relative expressions of these proteins, while these effects were reversed by quercetin (Fig. 3G and H). Moreover, quercetin treatment alone had no significant effect on cell morphology and pyroptosis related proteins (Supplemental Figs. 2A–C). These data indicated that quercetin treatment has an obviously protective effect on macrophage pyroptosis induced by ox-LDL.

### 3.4. Quercetin protects from oxidative stress induced by ox-LDL/HD in THP-1 macrophages and ApoE$^{-/-}$ mice

In order to investigate whether quercetin inhibited macrophage pyroptosis by improving oxidative stress, we quantified the induction of cytoplasmic and mitochondrial oxidative stress by ox-LDL treatment. Ox-LDL treatment increased both DCFH-DA and mitosox staining demonstrating an increase in cytoplasmic and mitochondrial ROS production, which was inhibited by quercetin (Supplemental Figs. 3A and B). The cellular content of GSH, SOD and MDA reflected the antioxidant capacity of macrophages. Ox-LDL treatment decreased GSH and SOD levels (Supplemental Figs. 3C and E) and increased the level of MDA (Supplemental Fig. 3D), all of which were reversed by quercetin treatment. Moreover, ox-LDL treatment induced a loss of mitochondrial membrane potential in THP-1 macrophages (Supplemental Figs. 3F and H), assayed by JC-1 staining. In addition, ox-LDL treatment induced the leakage of mtDNA. Supplemental Fig. 6G showed that the DNA in the

cytoplasm (in green) did not fully merge with mitochondrial staining (in red), indicative of mtDNA release out. To confirm that quercetin suppresses mtDNA leakage into cytoplasm, we quantified mtDNA in isolated cytosolic fractions by PCR. The results showed that significant enrichment in mtDNA in the cytosol under ox-LDL conditions compared with that in the control groups (Supplemental Fig. 3I). Quercetin treatment maintained mitochondrial membrane potential and significantly suppressed the leakage of mtDNA upon ox-LDL treatment, potentially as a result of the reduction of oxidative stress.

These observations were also replicated in vivo. Dihydroethidium (DHE) fluorescence quantification of oxidative stress showed that quercetin attenuated the oxidative stress in descending aorta compared to HD group (Supplemental Figs. 3J and K). In addition, quantification of SOD, GSH and MDA levels in the serum of ApoE$^{-/-}$ mice demonstrated that quercetin reversed the decreased GSH and SOD levels compared to the HD group (Supplemental Fig. 3M and N), and the increased MDA level observed in the HD group (Supplemental Fig. 3L). Taken together, these data demonstrated that quercetin protected macrophage from increased oxidative stress induced by ox-LDL, which were replicated in our in vivo model.

### 3.5. Quercetin enhanced cellular anti-oxidative effects and inhibits macrophage pyroptosis through activation of the KEAP1/NRF2 pathway

Immunofluorescence staining of NRF2 and western blot demonstrated that quercetin treatment enhanced the translocation of NRF2 into the nucleus (Fig. 4A–D). It can be observed from western blot that
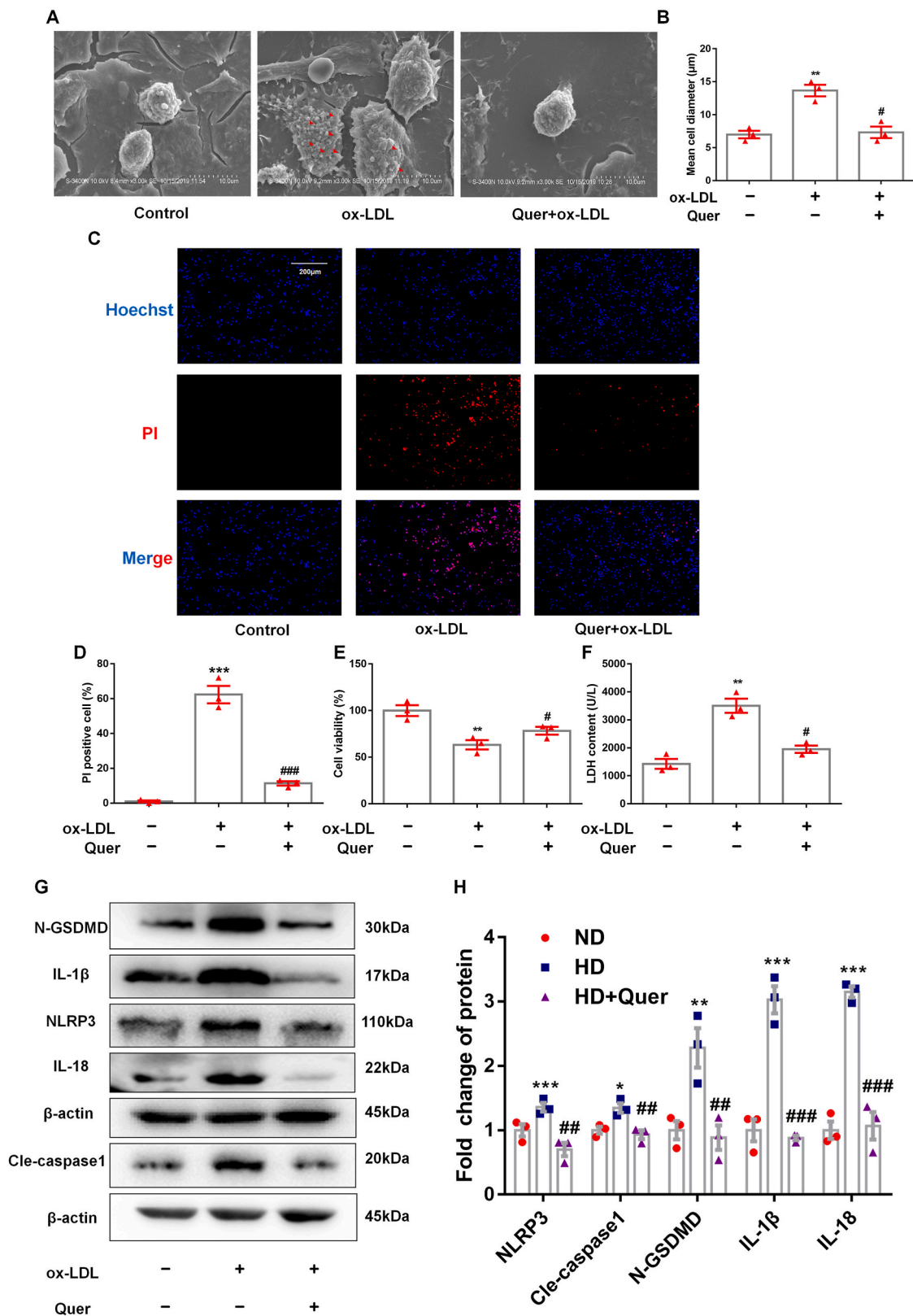
**Fig. 3.** Quercetin suppresses the pyroptosis of macrophage induced by ox-LDL.

THP-1 macrophages are pretreated with quercetin (50 μM) for 1 h, then stimulated with 100 μg/ml ox-LDL for 24 h. Scanning electron microscope, Hochest/PI staining, CCK-8 and LDH assay are used to evaluate the shape change and cell viability of macrophages in different groups, western blot is used to analyze the protein level of NLRP3 inflammasome. (A, B). Representative images for scanning electron microscope and the diameter of macrophage in different groups (n = 3 control vs n = 3 ox-LDL, **p < 0.01. n = 3 ox-LDL vs n = 3 ox-LDL + Quer, #p < 0.05). (C, D). Representative images and quantification of Hoechst/PI staining (n = 3 control vs n = 3 ox-LDL, ***p < 0.001. n = 3 ox-LDL vs n = 3 ox-LDL + Quer, ###p < 0.001). (E). CCK-8 (n = 3 control vs n = 3 ox-LDL, **p < 0.01. n = 3 ox-LDL vs n = 3 ox-LDL + Quer, #p < 0.05). (F). LDH assay (n = 3 control vs n = 3 ox-LDL, **p < 0.01. n = 3 ox-LDL vs n = 3 ox-LDL + Quer, #p < 0.05). (G, H). The NLRP3, N-GSDMD, cle-caspase1, IL-18, and IL-1β protein levels (n = 3, control vs ox-LDL group, *p < 0.05, **p < 0.01. n = 3 ox-LDL vs ox-LDL + Quer group, #p < 0.05).
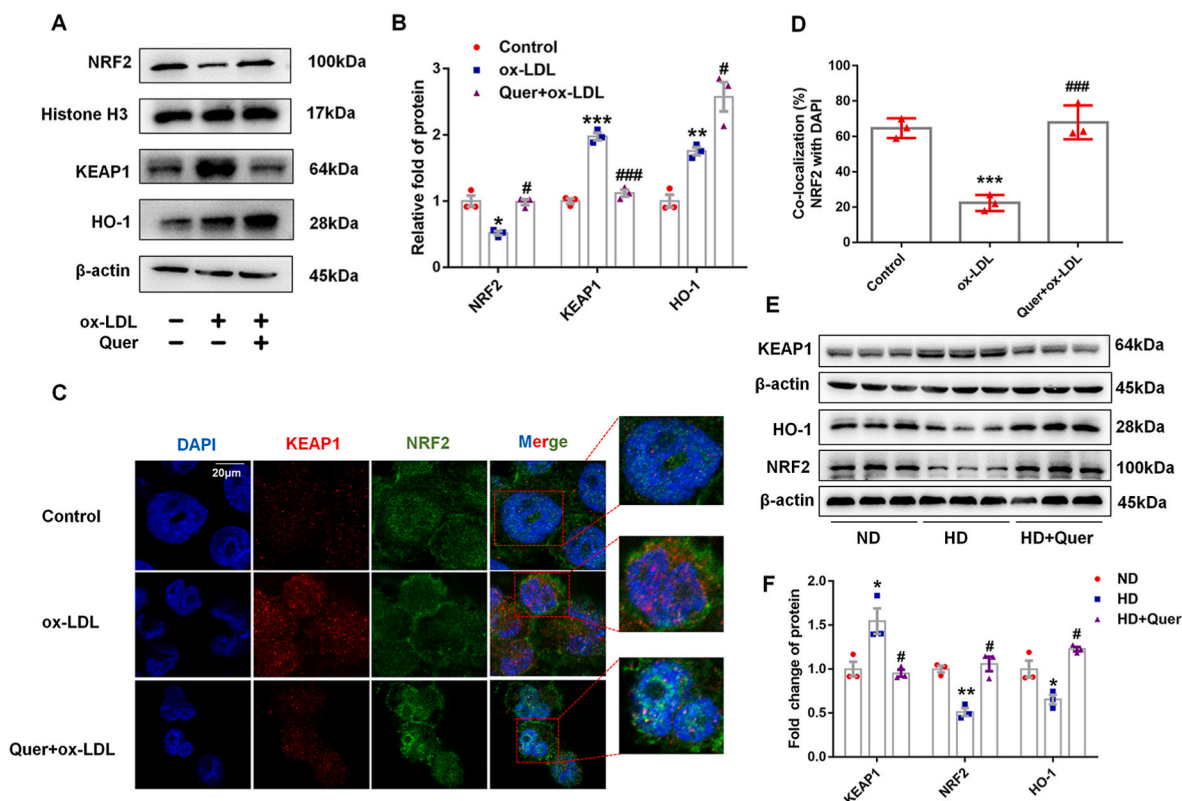
**Fig. 4.** Quercetin enhances NRF2 nuclear translocation and actives NRF2 pathway in macrophages and ApoE$^{-/-}$ mice.
In macrophages, the nuclear lysate was extracted to analysis NRF2 expression. In macrophages and aorta, total lysate was extracted to analysis KEAP1 and HO-1 expression. (A, B). Western blot is used to evaluate NRF2, KEAP1 and HO-1 levels (n = 3). (C, D). Confocal fluorescent staining is used to evaluate the nuclear translocation of NRF2 (n = 3). (E, F). The protein levels of NRF2, KEAP1 and HO-1 in the aorta of ApoE$^{-/-}$ mice (n = 3). *p < 0.05, **p < 0.01, ***p < 0.001, vs control or ND group. ##p < 0.01, ###p < 0.001, vs ox-LDL or HD group.

ox-LDL treatment increased the expression of KEAP1, which were reversed by quercetin treatment. Quercetin also increased HO-1 expression significantly (Fig. 4A and B). Similarly, the expression of NRF2 and HO-1 were decreased and KEAP1 was increased significantly in total aortic lysate of HD group, while quercetin mitigated these changes (Fig. 4E and F).

To confirm whether quercetin exerted its anti-oxidative effect via activating NRF2 pathway. ML385, a specific inhibitor of NRF2, was used to pre-treat macrophages. DCFH-DA and mitosox staining indicated that ML385 abrogated the inhibitory effect of quercetin on total and mitochondrial ROS production induced by ox-LDL in macrophages (Fig. 5A–D). Furthermore, ML385 also suppressed the increase of GSH and SOD, the decrease of MDA in quercetin treated group, respectively (Fig. 5G–I). These results suggested that the anti-oxidative effects of quercetin are mediated by activating NRF2 pathway. In addition, the results from Hoechst/PI staining, CCK-8 and LDH assay showed that ML385 abolished the anti-pyroptotic effect of quercetin in ox-LDL treated macrophages (Fig. 6A–D). Moreover, the inhibitory effect of quercetin on NLRP3 inflammasome was also abrogated by ML385 pretreatment (Fig. 6E and F), revealing that the anti-pyroptotic effect of quercetin was dependent on the activation of NRF2 pathway.

### 3.6. ROS scavenging reduced the ox-LDL dependent enhancement of inflammasome activation

Oxidative stress has been shown to enhance NLRP3 inflammasome activation [33]. The macrophages were incubated with N-Acetyl-L-cysteine (NAC) and mito-tempo, the scavenge cellular total ROS or mitochondrial ROS, respectively. The results demonstrated that NAC and mito-tempo suppressed the excessive ROS production induced by

ox-LDL treatment (Fig. 5A–D). In addition, both NAC and mito-tempo markedly decreased the expression of NLRP3, cle-caspase1 and N-GSDMD (Fig. 5E and F).

### 3.7. Quercetin promoted the dissociation of NRF2 and KEAP1 by competing with NRF2 to bind KEAP1

Furthermore, we investigated the mechanisms by which quercetin increases NRF2 activation by performing molecular docking. As a result, the molecular docking between KEAP1 and quercetin was performed at a binding ratio of 1:1, 1:2 and 1:3, respectively, and the 3D overview of them were shown in Supplemental Figs. 4A–C. According to the docking score of each ratio, we found that two molecules of quercetin matched with a higher amount of binding free energy (Fig. 7B). While three molecules of quercetin bind with KEAP1 protein, there are only two conformations displayed. Thus, the 1:2 ratio is taken as a model to structural analysis. As shown in Fig. 7A, the residues of Arg415, Arg483 and Ser555 formed an attractive charge or hydrogen bond with two molecules of quercetin. Moreover, the residues of Ser508, Tyr525, Gly509, Ala556, and Phe478 formed a van der Waals with the two molecules of quercetin. Thus, the molecular docking results indicated a possibility that the two molecules of quercetin may bind to the NRF2 binding site of KEAP1 and form a stable complex. Previous studies demonstrated that the amino site of Cys151, Cys273, Arg415, Arg483 and Ser508 in KEAP1 were involved in regulating the activity of NRF2 [17–19]. Our molecular docking results suggested quercetin interacted with residues Arg415, Arg483, Ser555, Ser508, Tyr525, Gly509, Ala556, and Phe478 in KEAP1 summarized in the Venn diagram to highlight the overlapping residues (Fig. 7C). Given that hydrogen bonds are much stronger than other interactions, we assumed that quercetin may
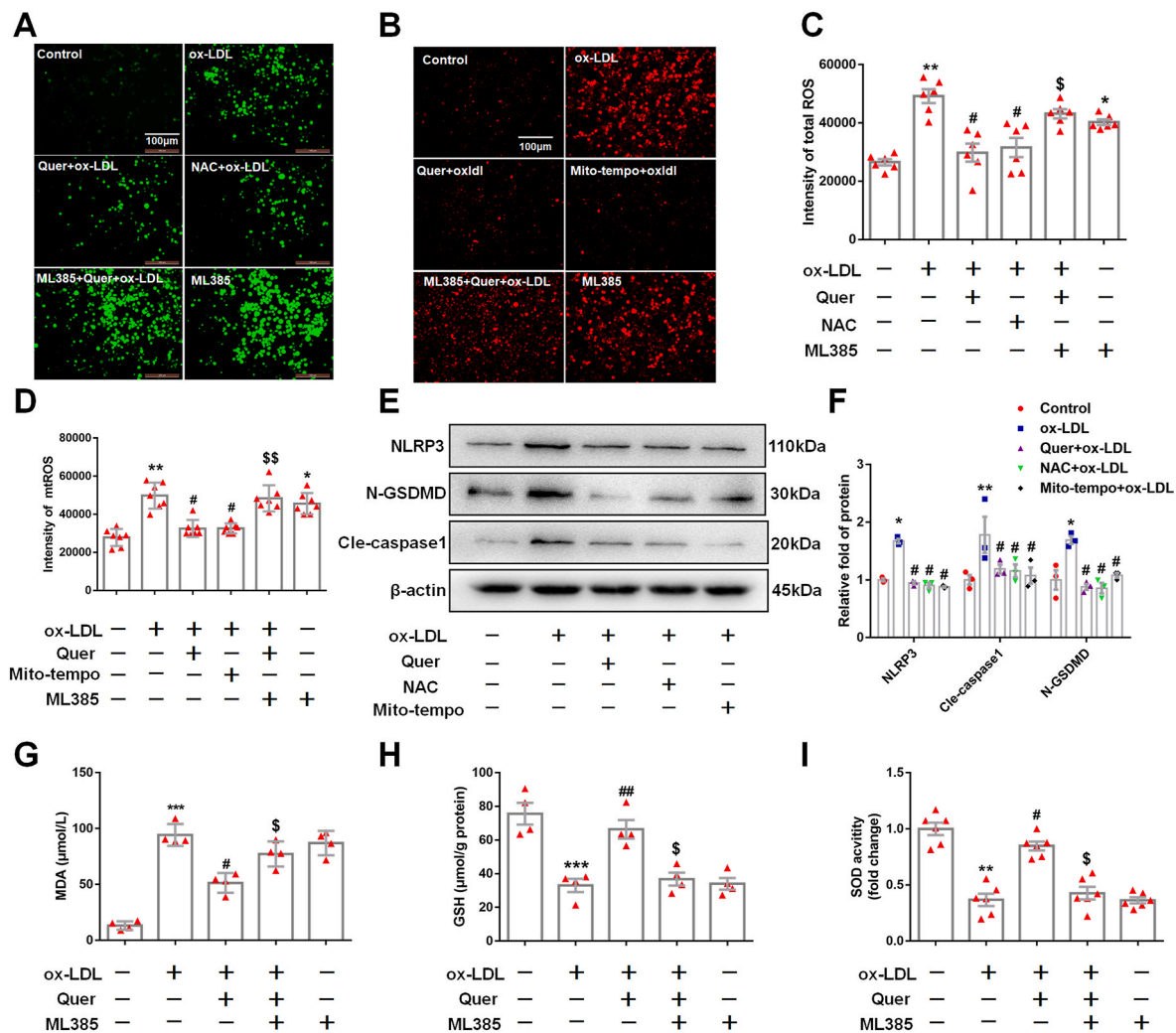
**Fig. 5.** ML385 abolishes the anti-ROS effect of quercetin.

5 μM ML385 was pretreated in 1 h, then 50 μM quercetin is added into the medium, after 1 h, 100 μg/ml ox-LDL is also added into the medium for 24 h. Immunofluorescence is used to observed the ROS staining, microplate reader is used to evaluated the intensity of ROS. The macrophages are divided into six groups, control groups, ox-LDL groups (ox-LDL, 100 μg/ml), Quer group (pretreated with 50 μM quercetin for 1 h, then combined with 100 μg/ml ox-LDL for 24 h), NAC group (pretreated with 10 μM NAC for 1 h, then combined with 100 μg/ml ox-LDL for 24 h), Mito-tempo group (pretreated with 10 μM mito-tempo for 1 h, then combined with 100 μg/ml ox-LDL for 24 h), ML385 group (5 μM ML385). Western blot is used to analyze the proteins of NLRP3, N-GSDMD and cle-caspase1. (A). Representative images for cellular ROS. (B). Representative images for mtROS. (C). Quantized data for cellular ROS (n = 6). (D). Quantized data for mitochondrial ROS (n = 7). (E, F). The expression of NLRP3, N-GSDMD, and cle-caspase1 (n = 3). (G). MDA level in control, ox-LDL, Quer + ox-LDL, ML385 (5 μM) + Quer + ox-LDL and ML385 (5 μM) group (n = 4). (H). GSH level in control, ox-LDL, Quer + ox-LDL, ML385 (5 μM) + Quer + ox-LDL and ML3853 (5 μM) group (n = 4). (I). SOD activity in control, ox-LDL, Quer + ox-LDL, ML3853 (5 μM) + Quer + ox-LDL and ML3853 (5 μM) group (n = 6). $*p < 0.05$, $**p < 0.01$, $***p < 0.01$ vs control group. $\#p < 0.05$, vs ox-LDL group. $\$p < 0.05$, $\$\$p < 0.01$ vs Quer + ox-LDL group.

competitively bind with the Arg415 and Arg483 sites of KEAP1 to promote the dissociation of NRF2 from KEAP1 (Fig. 7C).

### 3.8. Quercetin bound to KEAP1 at Arg483 with hydrogen bond to regulate NRF2 activity and improve oxidative stress

Co-immunoprecipitation of NRF2 with KEAP1 demonstrated that quercetin diminished the binding between NRF2 and its inhibitor KEAP1 in ox-LDL incubated macrophages (Fig. 8A). To verify our hypothesis that quercetin promoted NRF2 and KEAP1 dissociation by competitively binding with KEAP1 at Arg415 or Arg483, KEAP1 mutated at Arg415 or Arg483 to Serine (R415S or R483S) or wild type (WT) overexpression vectors were transfected into THP-1 macrophages (Fig. 9A). Immunoprecipitation was used to quantify the binding between NRF2 and mutated or wild-type KEAP1. The results demonstrated that quercetin promoted the dissociation between NRF2 and WT KEAP1 as well as

R415S mutated KEAP1, but not the R483S mutated KEAP1 (Fig. 8B). Moreover, transfection of R483S KEAP1 into macrophages prevented NRF2 nuclear translocation and the increase of HO-1 level in quercetin group (Fig. 8C–F). In addition, ROS, MDA and SOD level were significantly improved after quercetin treatment in macrophages transfected with WT or R415S KEAP1, but not in R483S KEAP1 transfected macrophages (Fig. 9B, G, H). Moreover, Hoechst/PI staining, CCK-8 and LDH assays demonstrated quercetin possessed anti-pyroptosis effect in macrophages transfected with WT and R415S KEAP1, but not in R483S KEAP1 mutation (Fig. 9C–F). Additionally, the protein structure of mutated KEAP1-R483S and KEAP1-WT were shown in Fig. 10A–C. The results demonstrated that KEAP1 with R483S mutation remained bound to NRF2 (Fig. 10D–F). The protein docking results showed that KEAP1-R483S interacted with NRF2 at a free energy of −19.4 kcal/mol, while KEAP1-WT interacted with NRF2 at a free energy of −192.1 kcal/mol (Table 1). These findings indicated that binding of quercetin to amino
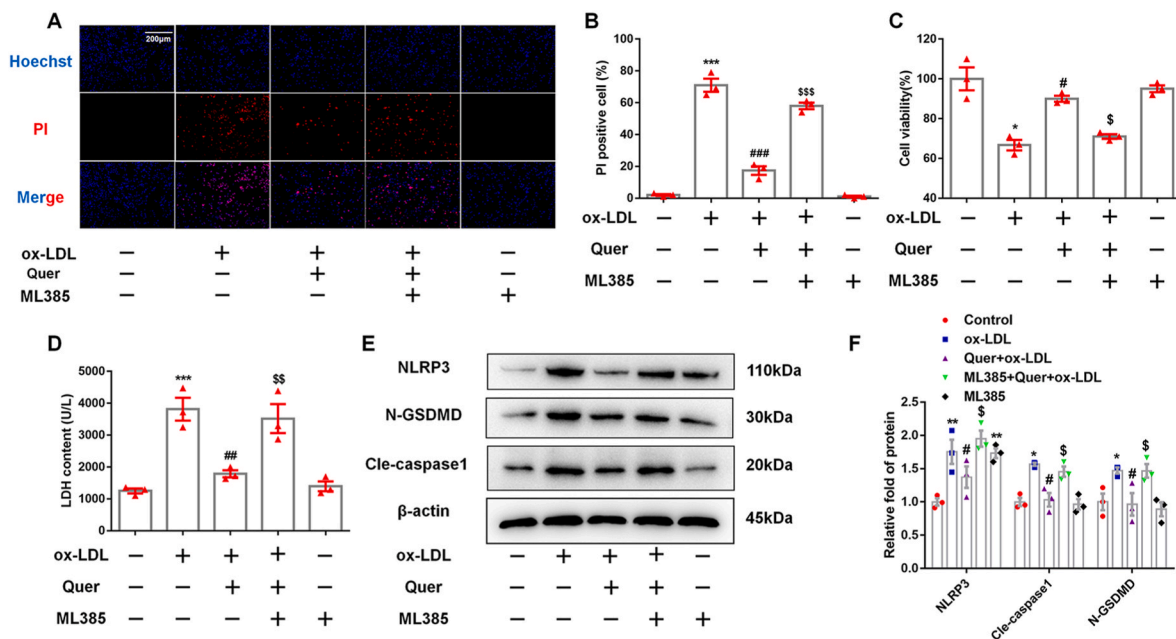
**Fig. 6.** ML385 abolishes the anti-pyroptotic effect of quercetin on macrophages.

5 μM ML385 was pretreated for 1 h, then 50 μM quercetin is added into the medium, after 1 h, 100 μg/ml ox-LDL is also added into the medium for 24 h. CCK-8, Hoechst/PI staining and LDH assay are used to evaluate the cell viability and cell membrane integrity, western blot is used to analyze the protein levels of NLRP3, cle-caspase1 and N-GSDMD. (A, B). Hoechst/PI staining (n = 3). Analyzed by Student's t-test. (C). CCK-8 (n = 3). Analyzed by Student's t-test. (D). LDH assay (n = 3), Analyzed by Student's t-test. (E, F). The NLRP3, cle-caspase1 and N-GSDMD protein levels (n = 3). *$p < 0.05$, **$p < 0.01$ vs control group. #$p < 0.05$, ##$p < 0.01$ vs ox-LDL group. $\$p < 0.05$ vs Quer + ox-LDL group.
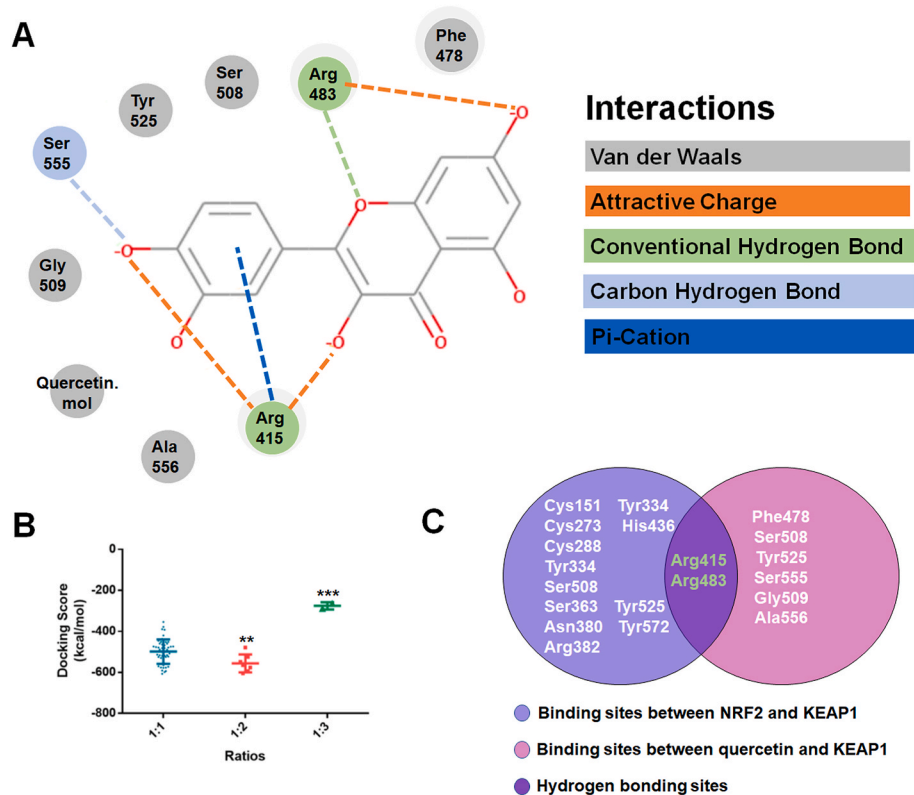


**Fig. 7.** The molecular docking study of quercetin and KEAP1.

(A). The residues detail of the interaction. (B). The docking score distributions for each ratio. (C). Venn diagram representing the overlap of the identified sites between NRF2/KEAP1 and quercetin/KEAP1. **$p < 0.01$, ***$p < 0.001$.

**Fig. 8.** Quercetin form hydrogen bond with KEAP1 at Arg483 to regulate NRF2 activity and reduce the generation of ROS in ox-LDL treated macrophages. Plasmid with mutated KEAP1 at R415S and R483S are transfected into macrophages, followed by quercetin (50 μM) treated for another 1 h. The macrophages lysates are immunoprecipitated with anti-KEAP1 antibody, and the immunoprecipitated proteins are used to immunoblot analysis with anti-NRF2 antibodies. The nuclear lysates are analyzed with anti–HO–1 and anti-histone H3 antibody. Anti-KEAP1 and anti-NRF2 are used for co-localized fluorescent staining. (A). Immunoprecipitation is used to detect the formation of NRF2 and KEAP1 complex (n = 3). (B–D). After quercetin treatment, immunoprecipitation and confocal fluorescent staining are used to detect the formation of NRF2 and KEAP1 complex and nuclear translocation of NRF2 in KEAP1-WT, KEAP1-R415S and KEAP1-R483S mutated macrophages (n = 3, ***$p < 0.001$, ox-LDL vs Quer + ox-LDL group). (E). Western blot is used to detect the NRF2 level in nuclear lysate (n = 3, *$p < 0.05$, vs control group. #$p < 0.05$, vs ox-LDL group). (F). Western blot is used to evaluate the HO-1 level in total lysate (n = 3, *$p < 0.05$, vs control group. #$p < 0.05$, vs ox-LDL group).
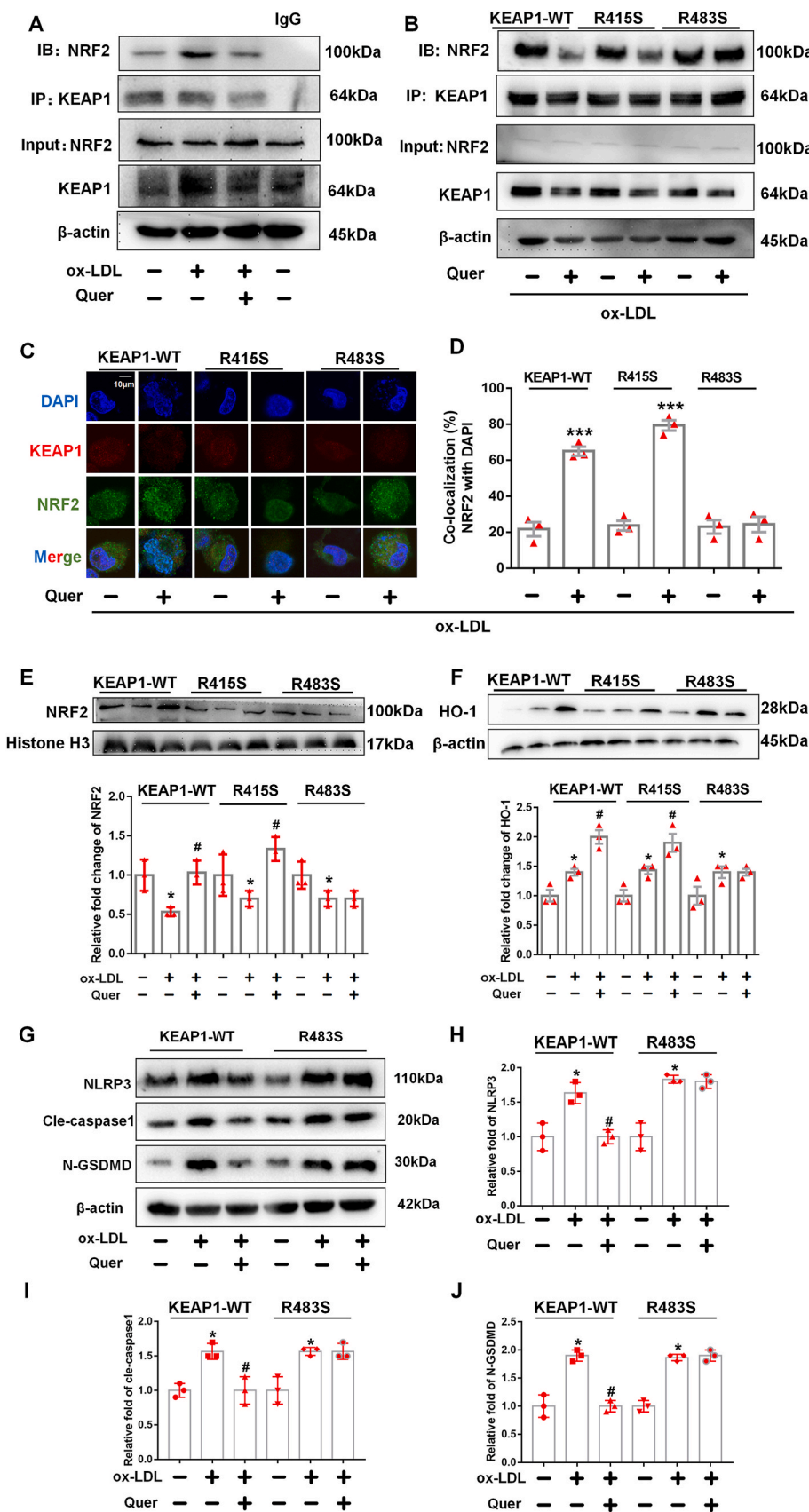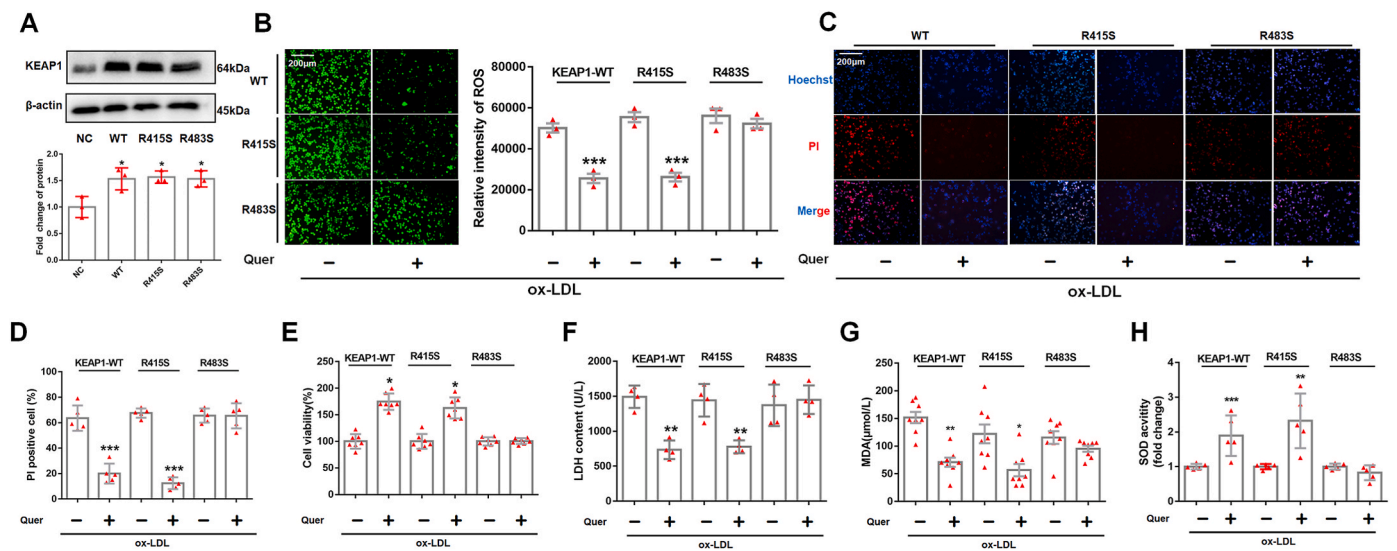
**Fig. 9.** The mutation of residue Arg483 in KEAP1 alleviates the anti-oxidative stress and anti-pyroptosis effect of quercetin pretreatment.
The plasmid with KEAP1-WT, single mutation at R415S or R483S are transfected into macrophages, quercetin (50 μM) is used to pre-treat macrophages, followed by ox-LDL (100 μg/ml) combined in different groups. (A). Western blot is used to evaluate the KEAP1 level in different groups (n = 3, *p < 0.05 vs NC group), Analyzed by Student's t-test. (B). DCFH-DA staining is used to display the ROS level in macrophages (n = 3), Analyzed by Student's t-test. (C–F). Hoechst/PI staining (n = 5), CCK-8 (n = 7) and LDH assay (n = 4) are used to measure the cell viability of macrophages (n = 5). Analyzed by Mann-Whitney *U* test. (G) The MDA level in macrophages (n = 8). Analyzed by Mann-Whitney *U* test. (H) The SOD activity in macrophages (n = 5). *p < 0.05, **p < 0.01, ***p < 0.001, vs ox-LDL group.
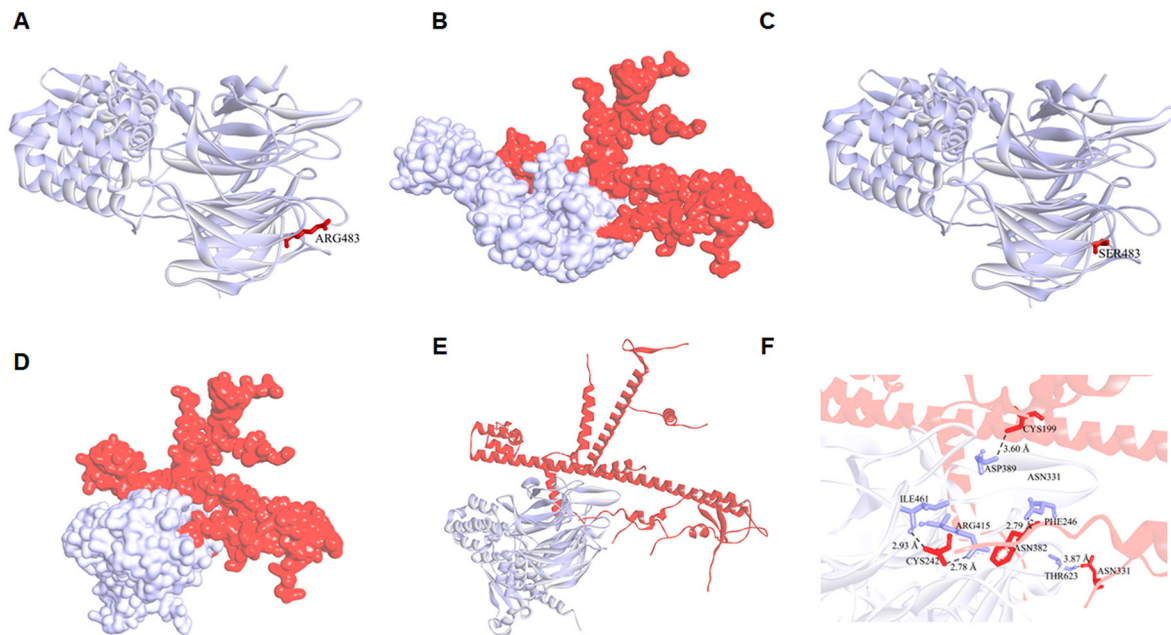


**Fig. 10.** Binding mode between KEAP1-R483S/KEAP1-WT and NRF2.
(A). Protein structure of KEAP1-WT. (B). Binding model between KEAP1-WT and NRF2. (C). Protein structure of KEAP1-R483S. (D, E). Binding model between KEAP1-R483S and NRF2. (F). The residues detail of the interaction between KEAP1-R483S and NRF2.

**Table 1**
KEAP1 and NRF2 binding free energy.

|  | Binding free energy (kcal/mol) |
| --- | --- |
| KEAP1-WT/NRF2 | −192.1 |
| KEAP1-R483S/NRF2 | −19.4 |

acid Arg483 in KEAP1 was critical for its ability to enable nuclear translocation of NRF2, improve oxidative stress and protect from pyroptosis in macrophages.

### 3.9. The atherosclerosis protective effect of quercetin was attenuated in ApoE$^{-/-}$ mice with AAV-KEAP1-R483S

To further confirm the protective effect of quercetin on atherosclerosis through competitive binding of KEAP1, AAV with KEAP1-WT and KEAP1-R483S were injected into 8 weeks ApoE$^{-/-}$ mice via tail vein. These mice were fed with HD supplemented with 0.1% (w/w) quercetin.
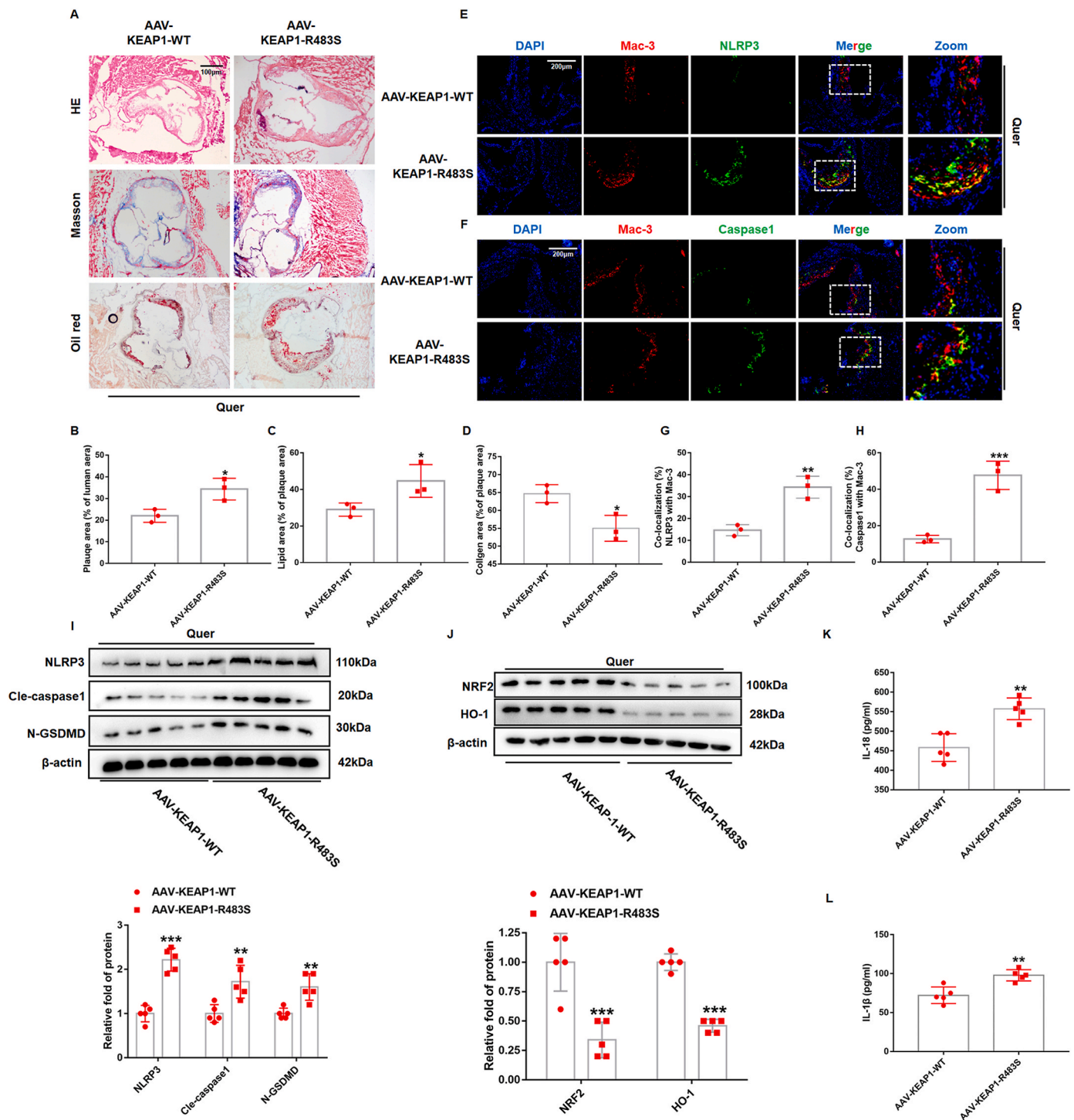
**Fig. 11.** Arg483 mutation weaks the protective effect of quercetin on atherosclerosis *in vivo*.

AAV-KEAP1-WT and AAV-KEAP1-R483S were injected intravenously through the tail of the mouse into 8-weeks-old ApoE$^{-/-}$ mice, all of which were given Quer diet. (A) Representative images for HE, Masson, and Oil red O stain. (B). Quantized data for HE staining (n = 3, *p < 0.05). (C). Quantized data for Oil red stain (n = 3, *p < 0.05). (D). Quantized data for Masson stain (n = 3, *p < 0.05). (E, G). NLRP3 and Mac-3 co-staining in aortic sinus (n = 3, **p < 0.01). (F, H). Caspase1 and Mac-3 co-staining in aortic sinus (n = 3, ***p < 0.001). (I, J) Western blot is used to evaluate NLRP3, Cle-caspase1, N-GSDMD, NRF2, and HO-1 levels (n = 5). **p < 0.01, ***p < 0.001. (K, L) The serum level of IL-18 and IL-1β (n = 5). **p < 0.01. . (For interpretation of the references to colour in this figure legend, the reader is referred to the Web version of this article.)

The results from HE and Oil Red-O staining demonstrated that plaque areas and lipid deposition area were significantly higher in AAV-KEAP1-R483S mice (Fig. 11A–C). Masson staining displayed that the area of collagen fiber decreased significantly in AAV-KEAP1-R483S mice (Fig. 11A, D). These results suggested that the atherosclerosis protective

effect of quercetin was attenuated in ApoE$^{-/-}$ mice with AAV-KEAP1-R483S. Furthermore, we performed immunofluorescence staining to evaluate NLRP3 and caspase1 levels in macrophages. It can be observed that the colocalization area of Mac-3 and NLRP3, caspase1 were significantly higher in AAV-KEAP1-R483S mice (Fig. 11E–H). Western

blot was used to analyze the expression of NLRP3, cle-caspase1, GSDMD, NRF2 and HO-1 in total lysate of artery. As we expected, the results showed that the protein level of NLRP3, cle-caspase1 and N-GSDMD were also increased in mice with AAV-KEAP1-R483S obviously (Fig. 11I), while the level of NRF2 and HO-1 were significantly decreased (Fig. 11J). The level of IL-1β and IL-18 in serum was also increased in mice with AAV-KEAP1-R483S (Fig. 11K and L).

## 4. Discussion

This study provided promising evidence that quercetin suppressed atherosclerosis by inhibiting macrophage pyroptosis via binding KEAP1 at Arg483 to release NRF2, which provided a new insight into the mechanisms of quercetin inhibiting atherosclerosis. Our data supported that quercetin, a typical natural antioxidant, suppressed atherosclerosis in ApoE$^{-/-}$ mice, partially by inhibiting macrophage pyroptosis and improving oxidative stress via enhancing NRF2 activation. In ox-LDL treated macrophages, quercetin reduced cellular and mitochondrial ROS level via promoting NRF2 nuclear translocation, consequently suppressed NLRP3 inflammasome mediated pyroptosis. The results from molecular docking and immunoprecipitation revealed that quercetin increased NRF2 dissociation from KEAP1 and enhanced NRF2 nucleus translocation by forming hydrogen bond with KEAP1 at Arg483 competitively. Furthermore, *in vivo* experiment demonstrated that the atherosclerosis protective effect of quercetin was attenuated in ApoE$^{-/-}$ mice with AAV-KEAP1-R483S.

In original cognition, pyroptosis was considered as a unique death form of monocytes, characterized by GSDMD mediated membranolysis and triggered by infection [41,42]. Since then, pyroptosis was found widely occurred in the initiation, progression and complications of atherosclerosis [41]. It was reported that hyperlipidemia promoted endothelial cells pyroptosis via activating caspase1 in HD fed ApoE$^{-/-}$ mice [43]. Moreover, exogenous stimuli such as nicotine and TMAO have also been found to promote endothelial cell pyroptosis *in vivo* and *in vitro* [44,45]. However, there is little evidence on the effects and underlying mechanism of macrophage pyroptosis in atherosclerosis. Accumulating studies have presented the crucial roles of macrophage death in the progression of atherosclerosis. Furthermore, it was reported that apoptotic macrophages in vulnerable plaques led to the increase of inflammatory response and plaque instability [34]. However, there are still lacking of attention on the effect and detailed mechanisms of macrophage pyroptosis in atherosclerosis.

Natural antioxidants, including quercetin, resveratrol and gallic acid, were widely used to study the protective effects of atherosclerosis. It was found that quercetin inhibited atherosclerosis through multiple mechanisms, such as improving endothelial cell dysfunction and suppressing dendritic cell activation [35]. It was also demonstrated that gallic acid attenuated atherosclerosis via suppressing smooth muscle cell proliferation and promoting cholesterol efflux. However, the mechanisms by which natural antioxidants protect against atherosclerosis still need further elucidation. In recent years, new theories of programmed cell death modalities have been proposed, especially pyroptosis, which has led to a further understanding of the mechanisms of atherosclerosis. Our previous work found that quercetin showed excellent protective ability against the typical macrophage pyroptosis model induced by LPS/ATP. Therefore, we speculated whether quercetin could inhibit atherosclerosis by suppressing macrophage pyroptosis. In the present study, our data demonstrated that quercetin inhibited macrophages pyroptosis in atherosclerotic plaques of ApoE$^{-/-}$ mice and suppressed the progression of atherosclerosis. *In vitro* experiment also showed that quercetin suppressed the macrophage pyroptosis induced by ox-LDL. Thus, our results suggested that inhibition of macrophage pyroptosis is also one of the potential mechanisms by which quercetin protects against atherosclerosis. Furthermore, we also found that quercetin inhibited macrophage pyroptosis by improving oxidative stress. There is considerable evidence demonstrating that oxidative stress is regarded as

a critical mechanism triggering NLRP3 inflammasome activation in pyroptosis [36,37]. The excessive ROS, as a danger-associated molecular pattern, was sensed by NLRP3 in cytoplasm and triggers the formation and activation of NLRP3 inflammasome. Varghese et al. found that ox-LDL induced NLRP3 inflammasome activation by promoting the ROS generation, and the induction of GSDMD oxidation was also considered to be one of the important mechanisms of pyroptosis caused by ROS [22]. Quercetin was well recognized for its multiple biological functions including anti-oxidation and anti-inflammation [38]. Indeed, our results were consistent with those results that quercetin significantly decreased the intracellular and mitochondrial ROS, and improved the loss of mitochondrial membrane potential in ox-LDL treated macrophages. Furthermore, we found that NAC and mito-temple significantly inhibited the activation of caspase1 and GSDMD, which is consistent with the results of quercetin treatment. These results suggested that quercetin may inhibit NLRP3 inflammasome activation and macrophage pyroptosis by inhibiting excessive ROS induced activation of GSDMD. Recent literature has reported the mechanism of ROS activation of inflammasome that ROS promoted the release of mitochondrial DNA into the cytoplasm, and mitochondrial DNA in cytoplasm binds to NLRP3, leading to the activation of NLRP3 inflammasome [39]. Furthermore, mitochondrial DNA-depleted macrophage (rhoO), showed significant resistance to ox-LDL induced pyroptosis [40]. In the present study, we also found quercetin markedly suppressed the release of mitochondrial DNA in macrophage pyroptosis. Taken together, these findings support that quercetin diminishes macrophage pyroptosis via inhibiting the ROS production, protecting from the dysfunction of mitochondrial and improving the release of mitochondrial DNA.

NRF2 was reported as a potent transcriptional activator, which regulates the transcription of numerous antioxidant genes in response to electrophilic and oxidative stress [41,42]. We observed that quercetin treatment increased NRF2 activity by enhancing NRF2 nuclear translocation and increasing the expression of HO-1, GSH and SOD in macrophages and ApoE$^{-/-}$ mice. Furthermore, in quercetin treated macrophages, ML385, pharmacological inhibitor of NRF2, significantly blocked the protective effects of quercetin on macrophage pyroptosis and oxidative stress. These data provided strong support for confirming that quercetin inhibited macrophage pyroptosis and attenuated atherosclerosis progression by activating NRF2 pathway. Previous studies have found that quercetin activated the NRF2 pathway through a variety of ways, including increasing NRF2 cell translocation, without affecting NRF2 expression or directly increasing NRF2 expression [43,44]. In our study, it was found that quercetin only increases NRF2 levels in the nucleus in macrophages, while *in vivo* study indicated that quercetin directly increased NRF2 levels in the aortic lysate, this difference may be related to differences between cells and tissues.

Previous studies have reported that quercetin can activate NRF2 pathway in several cell lines and tissues [43,44]. However, to the best of our knowledge, there is no data to elucidate the specific mechanism by which quercetin activates the NRF2 pathway. NRF2 activity was suppressed by interaction with the KEAP1/Cul3 ubiquitin ligase complex, KEAP1 association induces ubiquitination of NRF2 and resultant proteasomal degradation of NRF2 [27]. As a result, NRF2 activity was partly dependent on the binding between NRF2 and KEAP1, the Cys151, Arg415 and Arg483 sites of KEAP1 were found to play an important role in controlling NRF2 activity [45]. In recent years, it has been found that some molecules and proteins exerted antioxidant as well as anti-inflammatory effects by competitively binding KEAP1 with NRF2, leading to the dissociation of NRF2/KEAP1 and NRF2 pathway activation [46]. Ji and colleagues found that hydrogen sulfide improved oxidative stress in atherosclerosis and liver injury via S-sulfhydrated-KEAP1 at Cys151, which leads to the activation of NRF2 [42,47]. In the present study, quercetin was proved to suppress the expression of KEAP1 in macrophages, but we also found that quercetin activated the NRF2 pathway via binding to KEAP1 competitively. Rasha et al. and Wang et al. identified an inhibitory effect of quercetin on the protein

levels of KEAP1 in acute liver toxicity rat model and cadmium-induced oxidative damage cell model [48,49], which is similar to our results. These results suggested that quercetin may activate the NRF2 pathway through multiple mechanisms. In this study, we focused on the potential mechanism by which quercetin competitively bound to KEAP1 to increase NRF2 activity. We found quercetin promoted the dissociation of NRF2/KEAP1 complex and enhanced the expression of antioxidant protein. In order to better understand the mechanisms by which quercetin promoted the dissociation of NRF2 from KEAP1, we performed molecular docking to predict the binding site of quercetin and KEAP1. The results displayed that those two molecules of quercetin might bind to KEAP1 at Arg415 and Arg483 via conventional hydrogen bond, and these two sites were involved in the binding of KEAP1 to NRF2 [26,41]. To our surprise, rescue experiment demonstrated that the anti-oxidative stress and anti-pyroptosis effects of quercetin were only abolished in R483S mutated macrophages, but not in R415S macrophages. Furthermore, *in vivo* experiment showed that, the atherosclerosis and pyroptosis protective effects of quercetin were abolished in ApoE$^{-/-}$ mice with AAV-KEAP1-R483S. These results demonstrated that the binding of quercetin to the Arg483 site of KEAP1 is a key mechanism for its anti-atherogenic effect. To the best of our knowledge, the present study is the first to demonstrate that quercetin competitively bound to Arg483 in KEAP1 and ultimately activated NRF2 pathway in atherosclerosis.

In this study, Arg483 in KEAP1 was identified as a quercetin-binding site based on the current experiments with the Arg483 mutant, while there was still no significant improvement in NRF2 activity in Arg483 mutant macrophages compared to WT group. Interestingly, Lo et al. reported that KEAP1-R483A mutant is unable to bind to NRF2 and repress NRF2 activity [50], which is contradictory to our finding. We think there are several potential reasons to explain this. Firstly, Lo et al. transfected expression vectors for KEAP1 containing a C-terminal chitin binding domain (KEAP1-CBD) and mutant HA-NRF2 proteins into HEK 293T cells, and the expression of HA-NRF2 was detected in purified KEAP1-CBD lysate. However, there are still endogenous KEAP1 and NRF2 in HEK 293T cells, and this experiment excluded the expression of endogenous KEAP1 and NRF2. Secondly, Lo et al. mutated KEAP1-Arg483 into Ala483 in HEK 293T cells, while, in our study, KEAP1-Arg483 was mutated into Ser483 in THP-1 macrophages, which suggest that the differences in mutated amino acids and cell lines may contribute to the different results between the two experiments. Moreover, it is reported that, in neuron cell line, Arg415 mutation in KEAP1 has no significant influence the activity of NRF2 compared to WT group [51]. Thirdly, in Lo et al.' study, vectors for KEAP1-CBD and HA-NRF2 were transfected into HEK 293T cells without any other stimulations. However, in our study, the THP-1 macrophages were exposed to ox-LDL which might play a role in the interaction between KEAP1-R483S and NRF2. Furthermore, similar results have been reported in several other studies. For instance, Ji et al. found that exogenous hydrogen sulfide increased NRF2 activity by binding with the Cys151 site of KEAP1, but no significant improvement in NRF2 activity was observed in Cys151 mutate hepatocytes and macrophages incubated by ox-LDL [42,47].

In addition, we performed protein structure docking of KEAP1-R483S and NRF2. The results showed that although the Ser483 amino site in KEAP1-R483S no longer bounds to NRF2, while KEAP1-R483S still controlled the activity of NRF2. Moreover, the protein docking results showed that KEAP1-R483S interacted with NRF2 at a free energy of −19.4 kcal/mol, while KEAP1-WT interacted with NRF2 at a free energy of −192.1 kcal/mol (Table 1). The data indicated that although KEAP1-R483S can still bind to NRF2, the binding energy was substantially reduced, which suggested that the Arg483 mutation had little effect on the KEAP1/NRF2 binding state, but increased the instability of the KEAP1/NRF2 protein complex. Nevertheless, the potential mechanism by which KEAP1-R483S binds to NRF2 and represses NRF2 activity required further investigation.

## 5. Conclusions

Taken together, the mechanistic data clearly showed that quercetin suppressed atherosclerosis by inhibiting macrophage pyroptosis by improving oxidative stress, and the related mechanism is to promote NRF2 activation through binding to the Arg483 site of KEAP1 competitively. Therefore, this study provides new insights into the mechanisms by which quercetin protects against atherosclerosis.

## Authors' contributions

B. Y., J. L. and H. J.: Acquisition and Drafting the work. X. L. and X. W.: Acquisition of data for the work. X. B. and X. B., Y. L. and S. Z.: Analysis and interpretation of data. Y. C. and X. L.: Drafting the article. C.Z., M.Z., B.X., S. W. and T. J.: Revising the manuscript. All authors read and approved the final manuscript.

## Declaration of competing interest

The authors declare that they have no known competing financial interests or personal relationships that could have appeared to influence the work reported in this paper.

## Data availability

Data will be made available on request.

## Appendix A. Supplementary data

Supplementary data to this article can be found online at https://doi.org/10.1016/j.redox.2022.102511.

## References

[1] P. Libby, J.E. Buring, L. Badimon, G.K. Hansson, J. Deanfield, M.S. Bittencourt, et al., Atherosclerosis, Nat. Rev. Dis. Prim. 5 (2019) 56.
[2] H. Jinnouchi, Y. Sato, A. Sakamoto, A. Cornelissen, M. Mori, R. Kawakami, et al., Calcium deposition within coronary atherosclerotic lesion: implications for plaque stability, Atherosclerosis 306 (2020) 85–95.
[3] I. Tabas, K.E. Bornfeldt, Macrophage phenotype and function in different stages of atherosclerosis, Circ. Res. 118 (2016) 653–667.
[4] Z. Zhou, H. He, K. Wang, X. Shi, Y. Wang, Y. Su, et al., Granzyme A from cytotoxic lymphocytes cleaves GSDMB to trigger pyroptosis in target cells, Science (New York, NY) 368 (2020).
[5] K. Wang, Q. Sun, X. Zhong, M. Zeng, H. Zeng, X. Shi, et al., Structural mechanism for GSDMD targeting by autoprocessed caspases in pyroptosis, Cell 180 (2020) 941, 55.e20.
[6] V.A.K. Rathinam, Y. Zhao, F. Shao, Innate immunity to intracellular LPS, Nat. Immunol. 20 (2019) 527–533.
[7] S. Xu, H. Chen, H. Ni, Q. Dai, Targeting HDAC6 attenuates nicotine-induced macrophage pyroptosis via NF-κB/NLRP3 pathway, Atherosclerosis 317 (2021) 1–9.
[8] C. Mao, C. Li, E. Zhou, J. Zhang, C. Wang, C. Xue, Nicotine exacerbates atherosclerosis through a macrophage-mediated endothelial injury pathway, Aging 13 (2021) 7627–7643.
[9] J. Lin, X. Shou, X. Mao, J. Dong, N. Mohabeer, K.K. Kushwaha, et al., Oxidized low density lipoprotein induced caspase-1 mediated pyroptotic cell death in macrophages: implication in lesion instability? PLoS One 8 (2013), e62148.

[10] R.C. Coll, A.A. Robertson, J.J. Chae, S.C. Higgins, R. Muñoz-Planillo, M.C. Inserra, et al., A small-molecule inhibitor of the NLRP3 inflammasome for the treatment of inflammatory diseases, Nat. Med. 21 (2015) 248–255.

[11] A. Sharma, J.S.Y. Choi, N. Stefanovic, A. Al-Sharea, D.S. Simpson, N. Mukhamedova, et al., Specific NLRP3 inhibition protects against diabetes-associated atherosclerosis, Diabetes 70 (2021) 772–787.

[12] A. Grebe, F. Hoss, E. Latz, NLRP3 inflammasome and the IL-1 pathway in atherosclerosis, Circ. Res. 122 (2018) 1722–1740.

[13] G. Paramel Varghese, L. Folkersen, R.J. Strawbridge, B. Halvorsen, A. Yndestad, T. Ranheim, et al., NLRP3 inflammasome expression and activation in human atherosclerosis, J. Am. Heart Assoc. 5 (2016).

[14] F. Zheng, S. Xing, Z. Gong, Q. Xing, NLRP3 inflammasomes show high expression in aorta of patients with atherosclerosis. Heart, lung & circulation 22 (2013) 746–750.

[15] T. Hendrikx, M.L. Jeurissen, P.J. van Gorp, M.J. Gijbels, S.M. Walenbergh, T. Houben, et al., Bone marrow-specific caspase-1/11 deficiency inhibits atherosclerosis development in Ldlr(-/-) mice, FEBS J. 282 (2015) 2327–2338.

[16] J. Gage, M. Hasu, M. Thabet, S.C. Whitman, Caspase-1 deficiency decreases atherosclerosis in apolipoprotein E-null mice, Can. J. Cardiol. 28 (2012) 222–229.

[17] J. Yu, X. Cui, X. Zhang, M. Cheng, X. Cui, Advances in the occurrence of pyroptosis: a novel role in atherosclerosis, Curr. Pharmaceut. Biotechnol. (2020).

[18] Y. Pang, D. Wu, Y. Ma, Y. Cao, Q. Liu, M. Tang, et al., Reactive oxygen species trigger NF-κB-mediated NLRP3 inflammasome activation involvement in low-dose CdTe QDs exposure-induced hepatotoxicity, Redox Biol. 47 (2021), 102157.

[19] C. Zhang, M. Zhao, B. Wang, Z. Su, B. Guo, L. Qin, et al., The Nrf2-NLRP3-caspase-1 axis mediates the neuroprotective effects of Celastrol in Parkinson's disease, Redox Biol. 47 (2021), 102134.

[20] B. Zhou, J.Y. Zhang, X.S. Liu, H.Z. Chen, Y.L. Ai, K. Cheng, et al., Tom20 senses iron-activated ROS signaling to promote melanoma cell pyroptosis, Cell Res. 28 (2018) 1171–1185.

[21] J. Wang, M. Sahoo, L. Lantier, J. Warawa, H. Cordero, K. Deobald, et al., Caspase-11-dependent pyroptosis of lung epithelial cells protects from melioidosis while caspase-1 mediates macrophage pyroptosis and production of IL-18, PLoS Pathog. 14 (2018), e1007105.

[22] Y. Wang, P. Shi, Q. Chen, Z. Huang, D. Zou, J. Zhang, et al., Mitochondrial ROS promote macrophage pyroptosis by inducing GSDMD oxidation, J. Mol. Cell Biol. 11 (2019) 1069–1082.

[23] W. Lin, W. Wang, D. Wang, W. Ling, Quercetin protects against atherosclerosis by inhibiting dendritic cell activation, Mol. Nutr. Food Res. (2017) 61.

[24] P. Papakyriakopoulou, N. Velidakis, E. Khattab, G. Valsami, I. Korakianitis, N. P. Kadoglou, Potential pharmaceutical applications of quercetin in cardiovascular diseases, Pharmaceuticals 15 (2022).

[25] X. Luo, X. Bao, X. Weng, X. Bai, Y. Feng, J. Huang, et al., The protective effect of quercetin on macrophage pyroptosis via TLR2/Myd88/NF-κB and ROS/AMPK pathway, Life Sci. (2021), 120064.

[26] L. Baird, M. Yamamoto, The molecular mechanisms regulating the KEAP1-NRF2 pathway, Mol. Cell Biol. 40 (2020).

[27] E. Kansanen, S.M. Kuosmanen, H. Leinonen, A.L. Levonen, The Keap1-Nrf2 pathway: mechanisms of activation and dysregulation in cancer, Redox Biol. 1 (2013) 45–49.

[28] R. Xie, W. Zhao, S. Lowe, R. Bentley, G. Hu, H. Mei, et al., Quercetin alleviates kainic acid-induced seizure by inhibiting the Nrf2-mediated ferroptosis pathway, Free Radic. Biol. Med. 191 (2022) 212–226.

[29] K. Ren, T. Jiang, G.J. Zhao, Quercetin induces the selective uptake of HDL-cholesterol via promoting SR-BI expression and the activation of the PPARγ/LXRα pathway, Food Funct. 9 (2018) 624–635.

[30] S. Tedesco, F. De Majo, J. Kim, A. Trenti, L. Trevisi, G.P. Fadini, et al., Convenience versus biological significance: are PMA-differentiated THP-1 cells a reliable substitute for blood-derived macrophages when studying in vitro polarization? Front. Pharmacol. 9 (2018) 71.

[31] L. Zhou, Y.F. Zhang, F.H. Yang, H.Q. Mao, Z. Chen, L. Zhang, Mitochondrial DNA leakage induces odontoblast inflammation via the cGAS-STING pathway, Cell Commun. Signal. : CCS 19 (2021) 58.

[32] F. Berenger, A. Kumar, K.Y.J. Zhang, Y. Yamanishi, Lean-docking: exploiting ligands' predicted docking scores to accelerate molecular docking, J. Chem. Inf. Model. 61 (2021) 2341–2352.

[33] X. Le, J. Mu, W. Peng, J. Tang, Q. Xiang, S. Tian, et al., DNA methylation downregulated ZDHHC1 suppresses tumor growth by altering cellular metabolism and inducing oxidative/ER stress-mediated apoptosis and pyroptosis, Theranostics 10 (2020) 9495–9511.

[34] V. Simion, H. Zhou, S. Haemmig, J.B. Pierce, S. Mendes, Y. Tesmenitsky, et al., A macrophage-specific lncRNA regulates apoptosis and atherosclerosis by tethering HuR in the nucleus, Nat. Commun. 11 (2020) 6135.

[35] H. Duan, Q. Zhang, J. Liu, R. Li, D. Wang, W. Peng, et al., Suppression of apoptosis in vascular endothelial cell, the promising way for natural medicines to treat atherosclerosis, Pharmacol. Res. 168 (2021), 105599.

[36] D. Karunakaran, M. Geoffrion, L. Wei, W. Gan, L. Richards, P. Shangari, et al., Targeting macrophage necroptosis for therapeutic and diagnostic interventions in atherosclerosis, Sci. Adv. 2 (2016), e1600224.

[37] P. Wu, J. Chen, J. Chen, J. Tao, S. Wu, G. Xu, et al., Trimethylamine N-oxide promotes apoE(-/-) mice atherosclerosis by inducing vascular endothelial cell pyroptosis via the SDHB/ROS pathway, J. Cell. Physiol. 235 (2020) 6582–6591.

[38] O. Dagher, P. Mury, N. Thorin-Trescases, P.E. Noly, E. Thorin, M. Carrier, Therapeutic potential of quercetin to alleviate endothelial dysfunction in age-related cardiovascular diseases, Frontiers in cardiovascular medicine 8 (2021), 658400.

[39] S. Li, H. Li, Y.L. Zhang, Q.L. Xin, Z.Q. Guan, X. Chen, et al., SFTSV infection induces BAK/BAX-Dependent mitochondrial DNA release to trigger NLRP3 inflammasome activation, Cell Rep. 30 (2020) 4370–4385, e7.

[40] H. Yan, Y. Li, X. Peng, D. Huang, L. Gui, B. Huang, Resistance of mitochondrial DNA-depleted cells against oxidized low-density lipoprotein-induced macrophage pyroptosis, Mol. Med. Rep. 13 (2016) 4393–4399.

[41] M. Zhong, A. Lynch, S.N. Muellers, S. Jehle, L. Luo, D.R. Hall, et al., Interaction energetics and druggability of the protein-protein interaction between kelch-like ECH-associated protein 1 (KEAP1) and nuclear factor erythroid 2 like 2 (Nrf2), Biochemistry 59 (2020) 563–581.

[42] S. Zhao, T. Song, Y. Gu, Y. Zhang, S. Cao, Q. Miao, et al., Hydrogen sulfide alleviates liver injury through the S-Sulfhydrated-Kelch-Like ECH-associated protein 1/nuclear erythroid 2-related factor 2/low-density lipoprotein receptor-related protein 1 pathway, Hepatology 73 (2021) 282–302.

[43] W.M. Sayed, Quercetin alleviates red bull energy drink-induced cerebral cortex neurotoxicity via modulation of Nrf2 and HO-1, Oxid. Med. Cell. Longev. 2021 (2021), 9482529.

[44] M.Y. Hsu, Y.P. Hsiao, Y.T. Lin, C. Chen, C.M. Lee, W.C. Liao, et al., Quercetin alleviates the accumulation of superoxide in sodium iodate-induced retinal autophagy by regulating mitochondrial reactive oxygen species homeostasis through enhanced deacetyl-SOD2 via the nrf2-PGC-1α-sirt1 pathway, Antioxidants 10 (2021).

[45] P. Wang, J. Song, D. Ye, CRL3s: the BTB-CUL3-RING E3 ubiquitin ligases, Adv. Exp. Med. Biol. 1217 (2020) 211–223.

[46] D.A. Abed, M. Goldstein, H. Albanyan, H. Jin, L. Hu, Discovery of direct inhibitors of Keap1-Nrf2 protein-protein interaction as potential therapeutic and preventive agents, Acta Pharm. Sin. B 5 (2015) 285–299.

[47] L. Xie, Y. Gu, M. Wen, S. Zhao, W. Wang, Y. Ma, et al., Hydrogen sulfide induces keap1 S-sulfhydration and suppresses diabetes-accelerated atherosclerosis via Nrf2 activation, Diabetes 65 (2016) 3171–3184.

[48] R.M. Hussein, D.M. Sawy, M.A. Kandeil, H.S. Farghaly, Chlorogenic acid, quercetin, coenzyme Q10 and silymarin modulate Keap1-Nrf2/heme oxygenase-1 signaling in thioacetamide-induced acute liver toxicity, Life Sci. 277 (2021), 119460.

[49] J. Wang, K. Wang, L. Ding, P. Zhao, C. Zhang, H. Wang, et al., Alleviating effect of quercetin on cadmium-induced oxidative damage and apoptosis by activating the Nrf2-keap1 pathway in BRL-3A cells, Front. Pharmacol. 13 (2022), 969892.

[50] S.C. Lo, X. Li, M.T. Henzl, L.J. Beamer, M. Hannink, Structure of the Keap1:Nrf2 interface provides mechanistic insight into Nrf2 signaling, EMBO J. 25 (2006) 3605–3617.

[51] Y. Fang, J. Ye, B. Zhao, J. Sun, N. Gu, X. Chen, et al., Formononetin ameliorates oxaliplatin-induced peripheral neuropathy via the KEAP1-NRF2-GSTP1 axis, Redox Biol. 36 (2020), 101677.